

1
2
3 **CLIMATIC INDICES INFLUENCING THE LONG TERM VARIABILITY**
4 **OF MEDITERRANEAN HEAT AND WATER FLUXES:**
5 **THE NORTH ATLANTIC AND MEDITERRANEAN OSCILLATIONS**
6
7

8 *Francisco Criado-Aldeanueva⁽¹⁾, F. Javier Soto-Navarro⁽¹⁾, Jesús García-Lafuente⁽¹⁾*

9
10 *(1) Physical Oceanography Group, Department of Applied Physics II, University of Málaga,*
11 *Málaga, Spain.*
12
13
14
15
16

17 Corresponding author:

18 *Francisco Criado Aldeanueva*

19 *Dpto. Física Aplicada II, Universidad de Málaga*

20 *29071 Málaga, Spain*

21 *Tel.: +34 952 132849*

22 *fcaldeanueva@ctima.uma.es*
23
24

25 **CLIMATIC INDICES INFLUENCING THE LONG TERM VARIABILITY OF**
26 **MEDITERRANEAN HEAT AND WATER FLUXES: THE NORTH ATLANTIC**
27 **AND MEDITERRANEAN OSCILLATIONS**

28

29 **ABSTRACT:** Interannual to interdecadal precipitation (P), evaporation (E), water
30 deficit (E-P) and total heat flux have been correlated with North Atlantic Oscillation
31 (NAO) and Mediterranean Oscillation (MO) indices to explore the influence of large-
32 scale atmospheric forcing in the Mediterranean water and heat budgets variability.
33 Basin-averaged precipitation decrease from mid-60s to late-80s clearly corresponds to a
34 switch from a low to a high state of both indices. E-P variability is not so well
35 correlated with the atmospheric indices due to the different sensitiveness of E and P that
36 leads to correlations of opposite sign in the Eastern and Western sub-basins. The
37 effectiveness of NAO and MO indices is rather similar for P and E-P but the regional
38 MO index has turned out to be a more successful indicator of interdecadal evaporation
39 and net heat flux because from mid 70s to early 90s there is a considerable discrepancy
40 with NAO index. Since the MO centre remains rather steady, it influences most of the
41 Mediterranean all year round, then becoming more suitable for monitoring long term
42 water and (especially) heat budgets variability.

43

44 **Keywords:** Heat and water budgets, long-term variability, atmospheric forcing, climatic
45 indices, Mediterranean Sea.

46

47

48

49

50 **INTRODUCTION**

51

52 The Mediterranean Sea (Figure 1), a semi-enclosed basin that extends over 3000 km in
53 longitude and over 1500 km in latitude with an area of $2.5 \cdot 10^{12} \text{ m}^2$, communicates with
54 the Atlantic Ocean through the Strait of Gibraltar and with the Black Sea through the
55 Turkish Bosphorus and Dardanelles Straits. Semi-enclosed basins such as the
56 Mediterranean are suitable for the characterisation of heat and water fluxes since they
57 make a budget closure feasible. Evaporative losses (E) are not balanced by precipitation
58 (P) and river runoff (R) and an Atlantic inflow through the Strait of Gibraltar is
59 necessary to balance the freshwater and salt budgets. The circulation in the
60 Mediterranean Sea is influenced to a large extent by the heat and freshwater air-sea
61 exchanges which depend on the meteorological and oceanic conditions (Tsimplis et al.,
62 2006). The heat and water budgets play a key role in dense water formation and hence
63 in the Mediterranean Thermohaline Circulation (Bethoux et al., 1999). As a
64 consequence, they affect the characteristics of the Mediterranean water masses and then
65 may potentially influence the Atlantic Ocean circulation via changes in the properties of
66 the Mediterranean Outflow (Bethoux et al., 1999; Potter and Lozier, 2004; Artale et al.,
67 2005; Millot et al., 2006). For these reasons, the improvement of our knowledge of heat
68 and water budgets and their long-term variability is a challenge for the scientific
69 community of the Mediterranean region and is thought to be crucial to understand the
70 Mediterranean circulation and climate and their evolution under climate change.

71

72 -----Approximate location of Figure 1-----

73

74 A great number of studies have dealt with the Mediterranean heat (Bethoux, 1979;
75 Bunker et al., 1982; May, 1986; Garrett et al., 1993; Gilman and Garrett, 1994;
76 Castellari et al., 1998; Matsoukas et al., 2005; Ruiz et al., 2008; Sanchez-Gomez et al.,
77 2011; Criado-Aldeanueva et al., 2012) and water (Bethoux, 1979; Peixoto et al., 1982;
78 Bryden and Kinder, 1991; Harzallah et al., 1993; Gilman and Garrett, 1994; Castellari et
79 al., 1998; Angelucci et al., 1998; Béthoux and Gentili, 1999; Boukthir and Barnier,
80 2000; Mariotti et al., 2002; Mariotti, 2010; Sanchez-Gomez et al., 2011; Criado-
81 Aldeanueva et al., 2012) budgets but only in the recentmost ones, which use longer
82 datasets, the attention focused on the interannual variability and its forcing mechanisms.
83 For instance, Criado-Aldeanueva et al. (2012) report three different periods in the
84 precipitation and evaporation anomalies: from early 50s to late 60s, a positive trend is
85 observed that changes to negative until late 80s when it changes sign again. This
86 variability also reflects in the total heat flux exchanged between the ocean and
87 atmosphere and suggests a 40-year period multi-decadal oscillation related to long-term
88 atmospheric forcing that needs further investigation.

89

90 Indices of large-scale climate modes provide an integrated measure of weather linked
91 more to the overall physical variability of the system than to any individual local
92 variable. Among these indices, the North Atlantic Oscillation (NAO) is one of the most
93 prominent modes of the northern hemisphere climate variability (Walker and Bliss,
94 1932; van Loon and Rogers, 1978; Barnston and Livezey 1987; see Hurrell et al., 2003
95 for a recent review). It consists of a dipole of the sea level pressure over the North
96 Atlantic-European region with one centre reflecting the Iceland low and the other the
97 Azores high. Both phases of the NAO (stronger and weaker dipole) are associated with
98 basin-wide changes in the intensity and location of the North Atlantic jet stream and

99 storm track and in large-scale modulations of the normal patterns of zonal and
100 meridional heat and moisture transport, which in turn results in changes in temperature
101 and precipitation patterns over extended areas, including the Mediterranean sea (Walker
102 and Bliss 1932; van Loon and Rogers 1978; Rogers and van Loon 1979; Hurrell 1995;
103 Serreze et al., 1997; Dai et al., 1997; Mariotti et al., 2002; Mariotti and Arkin, 2007).
104 Interest in NAO has been recently renewed because a trend towards its positive phase,
105 especially in the last two or three decades, has been observed.

106

107 Although very important, NAO is not the only mode of variability of the northern
108 hemisphere: the Artic Oscillation (AO), defined as the first leading mode from the EOF
109 analysis of monthly mean height anomalies at 1000 hPa poleward of 20°N, is highly
110 correlated with NAO in the Atlantic region because of the overlap of their spatial
111 patterns in this sector and could be candidate for monitoring the large-scale atmospheric
112 forcing instead of NAO. But the results of Ambaum et al. (2002) show that the NAO
113 has a separated set of physical processes involved in its variability that makes it more
114 robust and physically relevant and has therefore been preferred for this study.

115

116 Conte et al (1989) suggested the possible existence of a Mediterranean Oscillation
117 (MO) as a consequence of the dipole behaviour of the atmosphere in the area between
118 the Western and Eastern Mediterranean. Differences in temperature, precipitation,
119 circulation and other parameters between both basins were attributed to this MO and an
120 index to measure the intensity of this dipole-like behaviour was proposed (Conte et al.,
121 1989; Kutiel et al., 1996; Maheras et al., 1999; Supic et al., 2004; Suselj and Bergant,
122 2006). Some aspects of the Mediterranean climate variability have been reported to be
123 better reflected by the MO index (Supic et al., 2004), including the flow exchange

124 through Gibraltar (Gomis et al., 2006). More recently, Papadopoulos et al. (2012) stated
125 that the MO index captures to a certain extent the influence of other independent modes
126 of low-frequency atmospheric variability such as the East Atlantic (EA), the East
127 Atlantic-West Russia (EA-WR) or the Scandinavian (SCAND) patterns over the
128 Mediterranean and hence provides a valuable measure of the atmospheric impact on the
129 basin.

130

131 In contrast to NAO, that has been extensively studied, only a few previous works focus
132 on the MO index and more research is required, especially to assess its influence in heat
133 and water budgets in the Mediterranean Sea, which is the objective of this work. To this
134 aim, we correlate interannual to interdecadal precipitation, evaporation, water deficit (E-
135 P) and total heat flux with atmospheric indices (NAO and MO) and perform a
136 composite analysis to establish the relative importance of their positive and negative
137 phases in the climatic variables. The work is organised as follows: section 2 describes
138 the data and methodology; section 3 presents and discuss the results both from a
139 regional and global approach and finally section 4 summarises the conclusions.

140

141 **DATA AND METHODOLOGY**

142

143 Since there is no unique way to describe the spatial structure of the NAO or MO, it
144 follows that there is no universally accepted index to describe the temporal evolution of
145 the phenomenon. Most recent NAO or MO indices are derived either from the simple
146 difference in surface pressure anomalies between various locations (Rogers, 1984;
147 Conte et al., 1989; Hurrell, 1995; Jones et al., 1997; Slonosky and Yiou, 2001; see Jones
148 et al., 2003 for a comparison between several station-based indices) or from the

149 Principal Components (PC) time series of the leading Empirical Orthogonal Function
150 (EOF) of sea level pressure or some other climate variable (Suselj and Bergant, 2006;
151 Gomis et al., 2006; Mariotti and Arkin, 2007; see Hurrell and Deser, 2010 for a review
152 of diverse methods). A disadvantage of the station-based indices is that they are fixed in
153 space and are significantly affected by small-scale and transient meteorological events
154 that introduce noise (Trenberth, 1984; Hurrell and van Loon, 1997) whereas the PC time
155 series approach is more optimal representation of the full spatial pattern (Hurrell and
156 Deser, 2010) and will be used in this work unless differently stated.

157

158 The monthly NAO index from the National Oceanic and Atmospheric Administration
159 (NOAA) Climate Prediction Center (CPC) has been retrieved. Its calculation is based on
160 the Rotated Principal Component Analysis (Barnston and Livezey, 1987) applied to
161 monthly mean standardized 500-mb height anomalies for 20°N-90°N (see
162 <http://www.cpc.ncep.noaa.gov/data/teledoc/teleindcalc.shtml> for a detailed description).

163 The MO pattern has been computed as the first PC mode of normalised sea level
164 pressure anomalies across the extended Mediterranean region (30°W-40°E in longitude,
165 30°N-60°N in latitude) which exhibits a single centre located over the Central and
166 Western Mediterranean (Figure 1), fairly steady in all seasons. The MO index is then
167 obtained as the corresponding time coefficients of the first PC mode. Since we define
168 the positive phase when sea level pressure anomaly above the Mediterranean is positive,
169 MO and NAO indices are positively correlated.

170

171 Monthly means from January 1948 to February 2009 of precipitation, evaporation and
172 surface heat fluxes have been retrieved from the National Center for Environmental
173 Prediction-National Center of Atmospheric Research (NCEP-NCAR) reanalysis project

174 (NCEP hereinafter, Kalnay et al., 1996), which is run at T62 spectral resolution
175 (approximately a grid size of 1.9°x1.9°) with 28 sigma levels. Auxiliary data of monthly
176 mean sea level pressure and air temperature at 2.5°x2.5° for the period 1948-2009 have
177 also been retrieved from NCEP database. Despite the uncertainties derived from the use
178 of reanalysis, Mariotti et al. (2002) showed that NCEP data exhibit good agreement
179 when compared with observational datasets at interannual to inter-decadal time scales in
180 the Mediterranean area. Moreover, the use of reanalysis allows the construction of
181 homogeneous time series (both in time and space), this leading to a better representation
182 of the basin-scale structures, which are the aim of this work. Seasonal means have been
183 computed by averaging JFM (winter), AMJ (spring), JAS (summer) and OND (autumn)
184 monthly data and Mediterranean spatially-averaged time series have been obtained by
185 averaging all grid points over the sea.

186

187 Linear correlation maps have been used to identify coupled patterns between the
188 climatic variables and the atmospheric NAO and MO indices. The statistical
189 significance of the correlation has been computed by transforming the correlation
190 matrix in a *t*-student distribution with N-2 degrees of freedom, where N is the number
191 of element of the analysed time series. Time filtering into low and high frequency
192 components is achieved using a 5-year running mean to take into account the long time
193 scale effects of the indices. Linear regression has also been used to quantify NAO (and
194 MO) related anomalies of the climatic variables. A complementary composite analysis
195 has also been performed to add robustness to the correlation results and highlight the
196 asymmetries between the positive and negative phases of the indices. First, we select
197 those years in which NAO and MO indices are in the upper (positive phase) and lower
198 (negative phase) quartiles over the period 1948-2009 and analyse their influence in the

199 climatic variables in terms of the average standard deviation anomalies during both
200 phases with respect to the complete time series on each grid point (Mariotti and Arkin,
201 2007). Only the points where the results are statistically different from zero (according
202 to a *t*-Student test at 95% significance) have been represented.

203

204 **RESULTS AND DISCUSSION**

205

206 *Precipitation*

207

208 Figure 2 displays the correlation between annual precipitation and winter NAO (panel
209 A) and annual MO (panel B) indices for the period 1948-2008. The most effective
210 (seasonal or annual) index will be selected for each variable hereinafter. A relatively
211 high (anti)correlation (above 0.5) is observed in the Algeric-Balearic and Aegean and
212 northern Levantine sub-basins (more evident for MO index). However, only in ~60% of
213 the Mediterranean, precipitation and atmospheric indices are significantly correlated on
214 annual basis with a mean absolute correlation, $|\text{corr}|$, about 0.4 (see table 1). The
215 correlation increases in winter (or even the entire rainy period, October-March),
216 especially for MO index, with wide regions close to -0.6 and a mean absolute value of
217 0.48 (not shown). Up to 80% of the basin (except the South-Eastern sub-basin) is
218 significantly correlated in this season, when P is generally linked to storm-track activity
219 captured by atmospheric indices. In summer, most of precipitation across the
220 Mediterranean region is of convective origin and is poorly correlated with the large-
221 scale atmospheric variability.

222

223 -----Approximate location of Figure 2-----

224

225 To further research the relationship between precipitation and the positive and negative
226 phases of the indices, we present now the composite analysis of Figure 3. During the
227 positive phase of the indices (panel A for NAO and C for MO), lower precipitation is
228 observed (up to -1.2 std anomalies). The NAO influence is more evident in the Western
229 Mediterranean and some areas of the Ionian whereas the MO is associated with a
230 noticeable reduction in precipitation in extensive areas of the whole basin. In the
231 negative phase (panels B for NAO and D for MO), higher precipitation is observed,
232 especially for the MO index, with values up to 1.2 std anomalies in the northern area.
233 NAO influence is not so evident in this state, the Levantine basin being the most
234 sensitive region.

235

236 -----Approximate location of Figure 3-----

237

238 Anti-correlation is expectable for P since the positive NAO phase (stronger dipole)
239 strengthens and modifies the orientation of prevailing westerly winds and associated
240 storm-track activity which cause increased precipitation over the northern Europe and
241 dry anomalies in the Mediterranean region (Hurrell, 1995; Serreze et al., 1997; Dai et
242 al., 1997). Roughly opposite conditions occur during the negative (weaker dipole) NAO
243 phase. The relation with the MO index is highlighted in Figure 4, where sea level
244 pressure anomalies are shown both for its positive (panel C) and negative (panel D)
245 phases. The positive phase is associated with higher than average pressure over the
246 Mediterranean, especially over the northern and eastern areas and hence lower
247 precipitation is expected. In contrast, the negative phase is linked with anomalously low
248 pressure over the whole basin and intense cyclogenesis over the Central/Western

249 Mediterranean that produces anomalously wet conditions over most of the
250 Mediterranean and, hence, negative correlation with P.

251

252 At decadal timescales (Figure 2C-D), the correlation considerably increases up to a
253 mean absolute value close to 0.6 (table 1) with extended regions (especially the Algeric-
254 Balearic and the Aegean and northern Levantine) highly correlated (~ -0.8) and a very
255 similar performance of both NAO and MO indices. This result confirms the importance
256 of the choice of a long period for budget studies in the Mediterranean, since the long
257 time scale effects of the indices must be taken into account because of their direct
258 implication on the climatic variables (Pettenuzzo et. al., 2010). The precipitation
259 anomalies resulting from the regression of precipitation with the NAO index (Figure 2E,
260 results for MO index are rather similar, not shown) indicates that, following positive
261 NAO index anomalies, the Mediterranean experiences a decrease in precipitation up to
262 150-200 mm/year in some regions, mostly restricted north of 35°N, a result already
263 mentioned by Mariotti et al. (2002).

264

265 -----Approximate location of Figure 4-----

266

267 Basin wide (Figure 2F), decadal to interdecadal variability of the Mediterranean
268 precipitation appears to be even more closely related to NAO and MO indices with
269 correlations of -0.8 and -0.78, respectively (table 1). In particular, the decrease from
270 mid-60s to late-80s corresponds to a switch from a low to a high state of the indices
271 (notice that $-NAO$ and $-MO$ indices have been plotted). These results are in good
272 agreement with those of Mariotti et al. (2002), who obtained (only for NAO) a

273 correlation of -0.51 and -0.84 for annual and decadal (5-year running means) variability,
274 respectively.

275

276 -----Approximate location of Table 1-----

277

278 *Evaporation*

279

280 On annual basis, evaporation is poorly correlated with winter NAO (Figure 5A) and
281 only the northern Levantine sub-basin seems to be sensitive to large-scale atmospheric
282 forcing. More success is observed for the summer MO index (Figure 5B) that, although
283 with a moderate correlation (between -0.3 and -0.5 in most regions and a mean absolute
284 value of 0.37, see table 1) influences 70% of the Mediterranean. Composite analysis for
285 the positive (panel A) and negative (panel B) phases of the MO index is displayed in
286 Figure 4. During its positive phase, lower than average evaporation is observed,
287 especially in the Western basin with values up to -1 std anomaly in the Tyrrhenian basin
288 but also in the Levantine basin with values between -0.6 to -0.8 std anomalies. During
289 the negative phase, higher than average evaporation is observed elsewhere but
290 especially in the Levantine basin (up to 1.4 std anomalies).

291

292 Anti-correlation is again expected since, with negative indices, anomalously low
293 pressure over the whole basin is observed (see Figure 4D) and colder and dryer air
294 masses from continental regions prevail, generating more severe weather conditions
295 over the Northern and Eastern Mediterranean. With this state, an intensification of
296 evaporative losses to the atmosphere is expected. Conversely, positive values of the
297 indices are associated with higher than average pressure over the Mediterranean and

298 North Africa (Figure 4C) that promote a shift of the wind trajectories toward lower
299 latitudes. Warmer and moister air masses are then conveyed toward the Mediterranean
300 leading to milder winters and a consequent decrease in the evaporative lost (Hurrell,
301 1995). But in autumn, when higher evaporation is observed (Mariotti et al., 2002;
302 Criado-Aldeanueva et al., 2012), the southern centre of NAO is rather far from the
303 Mediterranean and the regional MO index reflects more successfully local wind
304 trajectories that condition evaporation. It is interesting to notice that summer MO index
305 achieves the maximum correlation (although close values are obtained with the annual
306 MO index) because its positive and negative phases are associated with very different
307 sea level pressure anomaly patterns (Figure 4 C-D) during the year that determine the
308 wind trajectories and hence, evaporation. Since evaporation is higher in autumn and
309 winter, the atmospheric forcing in summer triggers, to a certain extent, its evolution in
310 the following months.

311

312 -----Approximate location of Figure 5-----

313

314 At decadal timescales, the correlation increases up to a mean absolute value about 0.55
315 (table 1) with higher values (-0.7 to -0.8) in the Levantine (both indices) and Tyrrhenian
316 (MO index) sub-basins (Figure 5C-D), again confirming the long time scale effects of
317 the indices on the climatic variables (Pettenuzzo et. al., 2010). But the difference
318 between NAO and MO influence remains evident (only 55% of the basin is sensitive to
319 NAO and more than 80% to MO). The evaporation anomalies resulting from the
320 regression with the indices (Figure 5E, only results for NAO index are shown) indicates
321 that only the Levantine sub-basin, where higher evaporation is observed (Mariotti et al.,

322 2002; Criado-Aldeanueva et al., 2012), experiences a considerable decrease in
323 evaporation (250-350 mm/year) as a consequence of +1 NAO index anomalies.
324
325 Basin wide (Figure 5F), decadal to interdecadal variability of the Mediterranean
326 evaporation is also better correlated to the regional MO index (see table 1). For instance,
327 from mid 70s to early 90s, there is a considerable discrepancy between NAO index and
328 E variability, which seems to be better captured by MO index.

329

330 *E – P freshwater deficit*

331

332 The annual freshwater deficit (E-P) is poorly correlated with atmospheric indices
333 (Figure 6A-B). Only a reduced area near Corsica and Sardinia and the Adriatic (for the
334 MO index) are positively correlated whereas the easternmost Levantine sub-basin is
335 negatively correlated. Seasonal correlations are more successful: for instance, winter
336 deficit is positively correlated with winter MO index with a mean value of 0.45 in most
337 of the Northern (above 35°N) Mediterranean (not shown), but winter only accounts for
338 20% of annual deficit (Criado-Aldeanueva et al., 2012).

339

340 At decadal timescales, a clear bi-modal pattern is observed both for NAO and MO
341 indices (Figure 6C-D): in the North-Central Mediterranean, E-P is positively correlated
342 (0.5-0.6) with the atmospheric forcing whereas in the Levantine sub-basin anti-
343 correlation is observed (close to -0.6). In accordance, regression analysis of NAO (and,
344 similarly MO, not shown) index with E-P also show an increment (decrement) in the
345 freshwater deficit in the Central (Levantine) sub-basins following +1 change (Figure
346 6E). This bi-modal behaviour can be explained based on the different sensitiveness of E

347 and P to the atmospheric forcing in those regions. In the Central basin, P is dominant
348 (compare Figures 2E and 5E) and changes in E-P follow those of $-P$ (hence, positive
349 correlation is expected). In contrast, the Levantine sub-basin is highly sensitive to E (see
350 Figure 5E) and changes in E-P follow those of E (hence, negative correlation).

351

352 -----Approximate location of Figure 6-----

353

354 Mediterranean-averaged decadal to interdecadal E-P variability (Figure 6F) is not well
355 correlated with the large atmospheric forcing (~ 0.25), probably due to this bi-modal
356 pattern. The correlation doubles (0.5 and 0.48 for NAO and MO indices, respectively) if
357 only the period from 1970 is considered (when a switch from a low to a high state of the
358 indices seems to be followed by an increase in E-P), in agreement with the results of
359 Mariotti et al. (2002), who report 0.18 from NCEP (1949-98) and 0.55 from ERA
360 (1980-93) data. Longer time series are necessary to elucidate the large scale
361 atmospheric relationship with the water deficit.

362

363 *Net heat flux*

364

365 The net heat budget consists of two radiation components (solar shortwave radiation
366 absorbed by the sea and longwave radiation emitted by the sea) and two turbulent
367 contributions (latent and sensible heat fluxes). Annual net heat flux is moderately (mean
368 absolute value close to 0.4) correlated with MO index (Figure 7A) in most parts of the
369 Mediterranean (except the Alboran, Adriatic and north Aegean sub-basins). Similar
370 results are found for NAO index but more extended areas (especially the southern
371 Ionian) are not significantly correlated (Figure 7B). Decadal variations are more

372 successfully correlated with both indices ($|\text{corr}| \sim 0.6$, see table 1) with higher values
373 close to -0.8 in the Levantine sub-basin (for NAO index, Figure 7C) and in the Central
374 Mediterranean (for MO index, Figure 7D). The composite analysis of Figure 8 reveals
375 that, during the positive phase of the indices (panel A for NAO and C for MO), ocean
376 heat losses are lower (especially for the MO index in most of the Western basin with
377 values up to -1 std anomalies). In the negative phase (panels B for NAO and D for MO),
378 ocean heat losses are higher. This anomaly is more evident in the Levantine and Aegean
379 sub-basins (higher than 1.2 std anomalies) under the negative MO phase.

380

381 The physical explanation for this is related to the wind trajectories that induce the sea
382 level pressure anomaly pattern in both MO phases: in the positive state (Figure 4C), the
383 dipole of high pressure anomaly over North Africa and Central Europe brings warmer
384 and moister air masses, especially to the Central and Western Mediterranean, that lead
385 to milder winters and a consequent heat loss decrease. In contrast, in the negative state
386 (Figure 4D), the dipole of anomalously low pressure over Central Europe and Turkey
387 brings colder and dryer air masses from continental regions towards the Mediterranean,
388 that merge in the Levantine and Aegean sub-basins, generating more severe weather
389 conditions and higher heat losses, especially in these areas.

390

391 -----Approximate location of Figure 7-----

392

393 As shown by Criado-Aldeanueva et al. (2012), fluctuations in the net heat flux closely
394 follow those of the latent heat, this contribution becoming the main source of
395 interannual variability. Since latent heat losses are directly related to evaporation,
396 similarity between Figure 5 and Figure 7 (and also between Figure 4A-B and Figure

397 8C-D) is expectable. However, better correlation is observed for net heat flux (see also
398 table 1) due to the other heat contributions that correlate well with the atmospheric
399 indices (especially the MO index, e.g. $|\text{corr}| = 0.52$ and 0.55 for long and shortwave
400 radiation, respectively, in more than 80% of the basin at annual timescales). Notice that
401 the sign of the correlation is negative because we have selected net heat flux positive
402 toward the atmosphere (the same as evaporation). The net heat flux anomalies resulting
403 from the regression with the indices (Figure 7E for NAO index and very similar for MO
404 index, not shown) reveal that, similarly to evaporation, the Levantine sub-basin is the
405 most sensitive to changes in the large-scale atmospheric forcing.

406

407 Basin wide (Figure 7F), decadal to interdecadal variability of the Mediterranean net heat
408 flux is better correlated to the regional MO index (table 1). As previously said, from
409 mid 70s to early 90s, there is a considerable discrepancy between NAO index and E
410 (and hence, net heat) variability, which seems to be better captured by MO index.

411

412 -----Approximate location of Figure 8-----

413

414 **4.- SUMMARY AND CONCLUDING REMARKS**

415

416 We have correlated interannual to interdecadal precipitation, evaporation, water deficit
417 (E-P) and total heat flux with climatic NAO and MO indices to explore the influence of
418 atmospheric forcing in the Mediterranean water and heat budgets variability. The
419 effectiveness of NAO and MO indices is rather similar for P and E-P but the regional
420 MO index has turned out to be a more successful indicator of interdecadal evaporation
421 and net heat flux (see table 1, in bold).

422

423 The indices exhibit considerable interannual and multi-decadal variability and
424 prolonged periods of both positive and negative phases of the pattern are common. The
425 positive phase of the indices is associated with higher than average pressure over the
426 Mediterranean and hence lower precipitation whereas the negative phase is linked with
427 anomalously low pressure over the whole basin that produces anomalously wet
428 conditions over most of the Mediterranean. Evaporation and net heat flux is related to
429 the wind trajectories that induce the sea level pressure anomaly pattern in both MO
430 phases (Figure 4 C-D): in the positive state, the dipole of high pressure anomaly over
431 North Africa and Central Europe brings warmer and moister air masses, especially to
432 the Central and Western Mediterranean, that lead to milder winters and a consequent
433 heat loss (and evaporation) decrease. In contrast, in the negative state, the dipole of
434 anomalously low pressure over Central Europe and Turkey brings colder and dryer air
435 masses from continental regions towards the Mediterranean, that merge in the
436 Levantine and Aegean sub-basins, generating more severe weather conditions and
437 higher heat (and evaporative) losses, especially in these areas.

438

439 The annual time series of NAO and MO indices are highly correlated (~ 0.6), this
440 indicating a close relationship between the indices due to the forcing of Atlantic low
441 systems on Mediterranean cyclogenesis (Trigo et al., 2002). The MO can be seen as an
442 oscillation of sea level pressure anomalies in the Central and Western Mediterranean, a
443 significant source of cyclogenesis. Since the occurrence of these cyclones is partially
444 linked with the activity of North Atlantic fronts governed by NAO, a high correlation is
445 expectable. In winter, the southern centre of the NAO is located closer to the
446 Mediterranean and, for this reason, the best correlation for all variables is always

447 observed for winter NAO index. But in summer and spring, the southern centre of the
448 NAO moves westward (Hurrell, 1995) and lower correlation is observed. In contrast,
449 the MO centre remains rather steady and it influences the Mediterranean all year round
450 (hence annual indices are preferred). Additionally, due to its effect in the Mediterranean
451 pressure field, the MO index captures to a certain extent the influence of other
452 independent modes of low-frequency atmospheric variability, especially the East
453 Atlantic (EA, $r = 0.43$ on annual basis) but also the East Atlantic-West Russia (EA-WR)
454 or the Scandinavian (SCAND) patterns during the cold part of the year (Papadopoulos
455 et al., 2012), and provides a valuable measure of the atmospheric impact on the basin,
456 then becoming, more suitable for monitoring long term water and (especially) heat
457 budgets variability.

458

459 **ACKNOWLEDGEMENTS**

460

461 This work has been carried out in the frame of the P07-RNM-02938 Junta de Andalucía
462 Spanish-funded project. JSN acknowledges a postgraduate fellowship from Conserjería
463 de Innovación Ciencia y Empresa, Junta de Andalucía, Spain. Partial support from
464 CTM2010-21229 (M. of Science and Technology) and P08-RNM-03738 (Junta de
465 Andalucía) Spanish-funded projects are also acknowledged. NCEP data have been
466 provided by the NOAA/OAR/ESRL PSD, Boulder, Colorado, USA, from their website
467 at <http://www.esrl.noaa.gov/psd/>.

468

469

470

471

472 **REFERENCES**

473

474 Angelucci, M. G., N. Pinardi, and S. Castellari, 1998. Air–sea fluxes from
475 operational analyses fields: Intercomparison between ECMWF and NCEP analyses over
476 the Mediterranean area. *Phys. Chem. Earth*, 23, 569–574.

477 Artale, V., Calmanti, S., Malanotte-Rizzoli, P., Pisacane, G., Rupolo, W. and
478 Tsimplis, M. (2005). Mediterranean climate variability. In: Lionello, P., Malanotte-
479 Rizzoli, P., Boscolo, R. (eds). Elsevier, pp 282-323.

480 Barnston, A.G. and Livezey, R.E., 1987. Classification, seasonality and
481 persistence of low-frequency atmospheric circulation patterns. *Mon. Weather Rev.* 115,
482 1083-1126.

483 Bethoux, J.P, 1979. Budgets of the Mediterranean Sea: their dependence on the
484 local climate and on the characteristics of Atlantic waters. *Ocean. Acta* 2, 157-163.

485 Bethoux, J.P. and Gentili B., 1999. Functioning of the Mediterranean Sea: Past
486 and Present Changes related to freshwater input and climatic changes. *J. Mar. Syst.* (20),
487 33-47.

488 Bethoux, J.P., Gentili, B. and Taillez, D. (1999). Warming and freshwater
489 budget change in the Mediterranean since the 1940s, their possible relation to the
490 greenhouse effect. *Geophys. Res. Lett* 25, 1023-1026.

491 Boukthir, M., and B. Barnier, 2000. Seasonal and inter-annual variations in the
492 surface freshwater flux in the Mediterranean Sea from the ECMWF re-analysis project.
493 *J. Mar. Syst.*, (24), 343–354.

494 Bryden, H. L., and T. H. Kinder, 1991b. Steady two-layer exchange through the
495 Strait of Gibraltar. *Deep-Sea Res.*, 38S, 445–463.

496 Bunker, A.F., Charnock, H., Goldsmith, R.A., 1982. A note on the heat balance
497 of the Mediterranean and Red Seas. *J. Mar. Res.* 40, 73-84, Suppl.

498 Castellari, S., Pinardi, N., Leaman K., 1998. A model study of air-sea
499 interactions in the Mediterranean Sea. *J. Mar. Sys.* 18, 89-114.

500 Conte, M., Giuffrida, A. and Tedesco, S., 1989. The Mediterranean Oscillation,
501 impact on precipitation and hydrology in Italy. Conference on Climate Water. Pub. of
502 the Academy of Finland, Helsinki, 121-137.

503 Criado-Aldeanueva, F., Soto-Navarro, J., García-Lafuente, J., 2012. Seasonal
504 and interannual variability of surface heat and freshwater fluxes in the Mediterranean
505 Sea: budgets and exchange through the Strait of Gibraltar. *International Journal of*
506 *Climatology*, 32, 286-302 doi: 10.1002/joc.2268.

507 Dai, A., Fung, I.Y., del Genio, A.D., 1997. Surface observed global land
508 precipitation variations during 1900-88. *J. Clim* 10, 2943-2962.

509 Garrett, C., Outerbridge, R., Thompson, K., 1993. Interannual variability in
510 Mediterranean heat and buoyancy fluxes. *J. Climate* 6, 900-910.

511 Gilman, C., Garrett, C., 1994. Heat flux parameterization for the Mediterranean
512 Sea: the role of atmospheric aerosols and constraints from the water budget. *J. Geophys.*
513 *Res.* 99 (C3), 5119-5134.

514 Gomis, D., Tsimplis, M.N., Martín-Míguez, B., Ratsimandresy, A.W., García-
515 Lafuente, J. and Josey, S.A., 2006. Mediterranean sea level and barotropic flow through
516 the Strait of Gibraltar for the period 1958-2001 and reconstructed since 1659. *J.*
517 *Geophys. Res.* 111, C11005 doi: 10.1029/2005JC003186.

518 Harzallah, A., D. L. Cadet, and M. Crepon, 1993. Possible forcing effects of net
519 evaporation, atmospheric pressure and transients on water transports in the
520 Mediterranean Sea. *J. Geophys. Res.*, 98 (C7), 12 341–12 350.

521 Hurrell, J.W., 1995. Decadal trends in the North Atlantic Oscillation – regional
522 temperatures and precipitation. *Science* 269(5224), 676-679.

523 Hurrell, J.W. and van Loon, H., 1997. Decadal variations in climate associated
524 with the North Atlantic Oscillation. *Clim. Change* 36, 301-326.

525 Hurrell, J.W., Kushnir, Y., Ottersen, G. and Visbeck, M., 2003. The North
526 Atlantic Oscillation: climate significance and environmental impact. *Geophys. Monogr.*
527 *Ser* 134, 279pp.

528 Hurrell, J.W. and Deser, C., 2010. North Atlantic climate variability: the role of
529 the North Atlantic Oscillation. *J. Mar. Sys.* 79, 231-244.

530 Jones, P.D., Jonsson, T. and Wheeler, D., 1997. Extension to the North Atlantic
531 Oscillation using early instrument pressure observations from Gibraltar and south-west
532 Iceland. *Int. J. Climatol.* 17, 1433-1450.

533 Jones, P.D., Osborn, T.J. and Briffa, K.R., 2003. Pressure-based measures of the
534 North Atlantic Oscillation (NAO), a comparison and assessment of changes in the
535 strength of the NAO and its influence on surface climate parameters. In *The North*
536 *Atlantic Oscillation: Climatic Significance and Environmental Impact*, *Geophys.*
537 *Monogr. Ser.*, vol. 134, edited by J. W. Hurrell et al., pp. 51–62, AGU, Washington, D.
538 C., doi:10.1029/134GM03.

539 Kalnay, E and co-authors (1996). The NCEP/NCAR 40-year reanalysis project.
540 *Bull. Amer. Meteor. Soc.*, 77:437-471.

541 Kutiel, H., Maheras, P. and Guika, S., 1996. Circulation indices over the
542 Mediterranean and Europe and their relationship with rainfall conditions across the
543 Mediterranean. *Theor. Appl. Climatol.* 54, 125-138.

544 van Loon, H. and Rogers, J.C., 1978. The see-saw of winter temperatures
545 between Greenland and northern Europe. Part I: general descriptions. *Mon. Weather*
546 *Rev* 106, 296-310.

547 Maheras, P., Xoplaki, E. and Kutiel, H., 1999. Wet and dry monthly anomalies
548 across the Mediterranean basin and their relationship with circulation 1860-1990.
549 *Theor. Appl. Climatol* 64, 189-199.

550 Mariotti, A., Struglia, M.V., Zeng, N., Lau, K.-M., 2002. The hydrological cycle
551 in the Mediterranean region and implications for the water budget of the Mediterranean
552 Sea. *Journal of Climate* 15, 1674–1690.

553 Mariotti, A. and Arkin, P., 2007. The North Atlantic Oscillation and oceanic
554 precipitation variability. *Clim. Dyn* 28, 35-51.

555 Mariotti A, 2010. Recent Changes in the Mediterranean Water Cycle: A
556 Pathway toward Long-Term Regional Hydroclimatic Change? *Journal of Climate* 23
557 (6), 1513-1525.

558 Matsoukas, C., Banks, A. C., Hatzianastassiou, N., Pavlakis, K. G.,
559 Hatzidimitriou, D., Drakakis, E., Stackhouse, P. W., Vardavas, I., 2005. Seasonal heat
560 budget of the Mediterranean Sea. *J. Geophys. Res.*, 110, C12008,
561 doi:10.1029/2004JC002566.

562 May, P.W., 1986. A brief explanation of Mediterranean heat and momentum
563 flux calculations. NORDA code 322, NSTL, MS 39529.

564 Millot, C., Candela, J., Fuda, J.L. and Tber, Y. (2006). Large warming and
565 salinification of the Mediterranean outflow due to changes in its composition. *Deep-Sea*
566 *Res.* 53, 656-666.

567 Papadopoulos, V., Josey, S.A., Bartzokas, A., Somot, S., Ruiz, S. and
568 Drakopoulou, P. (2012). Large-scale atmospheric circulation favoring deep -and
569 intermediate- water formation in the Mediterranean Sea. *J. Climate* 25, 6079-6091.

570 Peixoto, J. P., M. De Almeida, R. D. Rosen, and D. A. Salstein, 1982.
571 Atmospheric moisture transport and the water balance of the Mediterranean Sea. *Water*
572 *Resour. Res.*, 18, 83–90.

573 Pettenuzzo, D., Large, W.G. and Pinardi, N. (2010). On the corrections of ERA-
574 40 surface flux products consistent with the Mediterranean heat and water budgets and
575 the connection between basin surface total heat flux and NAO. *J. Geophys. Res.* 115,
576 C06022, doi: 10.1029/2009JC005631.

577 Potter, R. and Lozier, S. (2004). On the warming and salinification of the
578 Mediterranean outflow waters in the North Atlantic. *Geophys. Res. Lett* 31, L01202.
579 doi: 10.1029/2003GL018161.

580 Rogers, J.C. and van Loon, H., 1979. The see-saw of winter temperatures
581 between Greenland and northern Europe. Part II: some oceanic and atmospheric effects
582 in middle and high latitudes. *Mon. Weather Rev* 107, 509-519.

583 Rogers, J.C., 1984. The association between the North Atlantic Oscillation and
584 the Southern Oscillation in the northern hemisphere. *Mon. Weather Rev.* 112 1999-
585 2015.

586 Ruiz S., Gomis D., Sotillo M. G., Josey S. A., 2008. Characterization of surface
587 heat fluxes in the Mediterranean Sea from a 44-year high-resolution atmospheric data
588 set. *Global and Planetary change*, (63), 256-274.

589 Sanchez-Gomez, E., Somot, S., Josey, S.A., Dubois, C., Elguindi, N. and Déqué,
590 M. (2011). Evaluation of Mediterranean Sea water and heat budgets simulated by an
591 ensemble of high resolution regional climate models. *Clim. Dyn.* 37, 2067-2086.

592 Serreze, M.C., Carse, F., Barry, R.G. and Rogers, J.C., 1997. Icelandic low
593 cyclone activity: climatological features, linkages with the NAO and relationships with
594 recent changes in the northern hemisphere circulation. *J. Clim* 10(3), 453-464.

595 Slonosky, V.C. and Yiou, P., 2001. Secular changes in the North Atlantic
596 Oscillation and its influence on 20th century warming. *Geophys. Res. Lett.* 28, 807-810.

597 Supic, N., Grbec, B., Vilibic, I. and Ivancic, I., 2004. Long-term changes in
598 hydrographic conditions in northern Adriatic and its relationship to hydrological and
599 atmospheric processes. *Annales Geophysicae* 22, 733-745.

600 Suselj, K. and Bergant, K., 2006. Mediterranean Oscillation Index. *Geophys.*
601 *Res. Abstr.* 8, 02145 European Geosciences Union.

602 Trenberth, K.E., 1984. Signal versus noise in the Southern Oscillation. *Mon.*
603 *Weather Rev.* 112, 326-332.

604 Trigo, I.F., Bigg, G.R. and Davies, T.D. (2002). Climatology of cyclogenesis
605 mechanisms in the Mediterranean. *Monthly Weather Review* 130 (3), 549-569.

606 Tsimplis, M., Zervakis, V., Josey, S. A., Peneva, E.L., Struglia, M.V., Stanev,
607 E., Teocharis, A., Lionello, P., Malanotte-Rizzoli, P., Artale, V., Tragou, E. and Orguz,
608 T. (2006). Changes in the oceanography of the Mediterranean Sea and their link to
609 climate variability. In: Lionello, P., Malanotte-Rizzoli, P., Boscolo, R. (eds). Elsevier,
610 pp 226-281.

611 Walker, G.T. and Bliss, W.E., 1932. World Weather V. *Memories of the Royal*
612 *Meteorological Society* 44, 53-84.

613
614
615
616

617 **FIGURE CAPTIONS**

618

619 **Table 1:** Mean absolute correlation, $|\text{corr}|$, at 95% significance level between annual
620 and decadal (5-years running means) NAO and MO indices and P, E, E-P and net heat
621 flux (Q). The fraction of points significantly correlated is shown in brackets. The last
622 two columns display the correlation between the indices and the Mediterranean-
623 averaged variables at decadal (5-years running means) timescales (time series of panel F
624 of Figures 2, 5-7). The best correlated seasonal index is indicated (w: winter, s: summer,
625 a: annual). Better results of MO index compared to NAO are highlighted in bold.

626

627 **Figure 1:** Map of the Mediterranean Sea. The main basins and sub-basins are indicated.
628 The MO pattern (contours) has been computed as the first PC of normalised sea level
629 pressure anomalies across the extended Mediterranean region (30°W-40°E, 30°N-60°N).

630

631 **Figure 2:** Correlation (95% significance) between precipitation (P) and large-
632 atmospheric indices for the period 1948-2008. A) Annual P and winter NAO index; B)
633 Annual P and MO index; C) 5-year running means of P and winter NAO index; D) 5-
634 year running means of P and MO index. E) Regression of P with winter NAO index at
635 decadal (5-year running means) timescales; F) Time series of 5-year running means of
636 winter -NAO (upper, green) and annual -MO (lower, red) indices and Mediterranean-
637 averaged P.

638

639 **Figure 3:** Composites of precipitation standard anomalies associated to the positive
640 (upper quartile) and negative (lower quartile) phases of winter NAO and MO indices for
641 the 60-year 1948-2008 period. A) Positive winter NAO; B) Negative winter NAO; C)

642 Positive MO; D) Negative MO. Only the points where the results are statistically
643 different from zero (according to a *t*-Student test at 95% significance) have been
644 represented.

645

646 **Figure 4:** Composites of evaporation standard anomalies (panels A-B) and sea level
647 pressure anomalies (hPa, panels C-D) associated to the positive (upper quartile, left
648 panels) and negative (lower quartile, right panels) phases of summer MO index for the
649 60-year 1948-2008 period. For evaporation, only the points where the results are
650 statistically different from zero (according to a *t*-Student test at 95% significance) have
651 been represented.

652

653 **Figure 5:** The same as Figure 2 for evaporation. The best correlated summer MO index
654 has been selected for correlations with this variable.

655

656 **Figure 6:** The same as Figure 2 for freshwater deficit E-P. Notice that positive NAO
657 and MO indices have been plotted in panel F.

658

659 **Figure 7:** The same as Figure 2 for net heat flux Q. The best correlated summer MO
660 index has been selected for correlations with this variable.

661

662 **Figure 8:** Composites of net heat flux standard anomalies associated to the positive
663 (upper quartile) and negative (lower quartile) phases of winter NAO and summer MO
664 indices for the 60-year 1948-2008 period. A) Positive winter NAO; B) Negative winter
665 NAO; C) Positive summer MO; D) Negative summer MO. Only the points where the

666 results are statistically different from zero (according to a *t*-Student test at 95%
 667 significance) have been represented.

668

669

670

671

672 **TABLES**

673

	Annual means		5-years means		5-years Med-averaged	
	NAO index	MO index	NAO index	MO index	NAO index	MO index
P	0.40 (54%)	0.45 (56%)	0.58 (82%)	0.56 (80%)	w -0.8	a -0.78
E	0.37 (36%)	0.37 (68%)	0.53 (55%)	0.55 (83%)	w -0.48	s -0.63
E-P	0.38 (38%)	0.39 (38%)	0.50 (60%)	0.48 (59%)	w 0.25	a 0.22
Q	0.39 (55%)	0.37 (74%)	0.56 (83%)	0.59 (93%)	w -0.63	s -0.70

674

675 **Table 1:** Mean absolute correlation, |corr|, at 95% significance level between annual
 676 and decadal (5-years running means) NAO and MO indices and P, E, E-P and net heat
 677 flux (Q). The fraction of points significantly correlated is shown in brackets. The last
 678 two columns display the correlation between the indices and the Mediterranean-
 679 averaged variables at decadal (5-years running means) timescales (time series of panel F
 680 of Figures 2, 5-7). The best correlated seasonal index is indicated (w: winter, s: summer,
 681 a: annual). Better results of MO index compared to NAO are highlighted in bold.

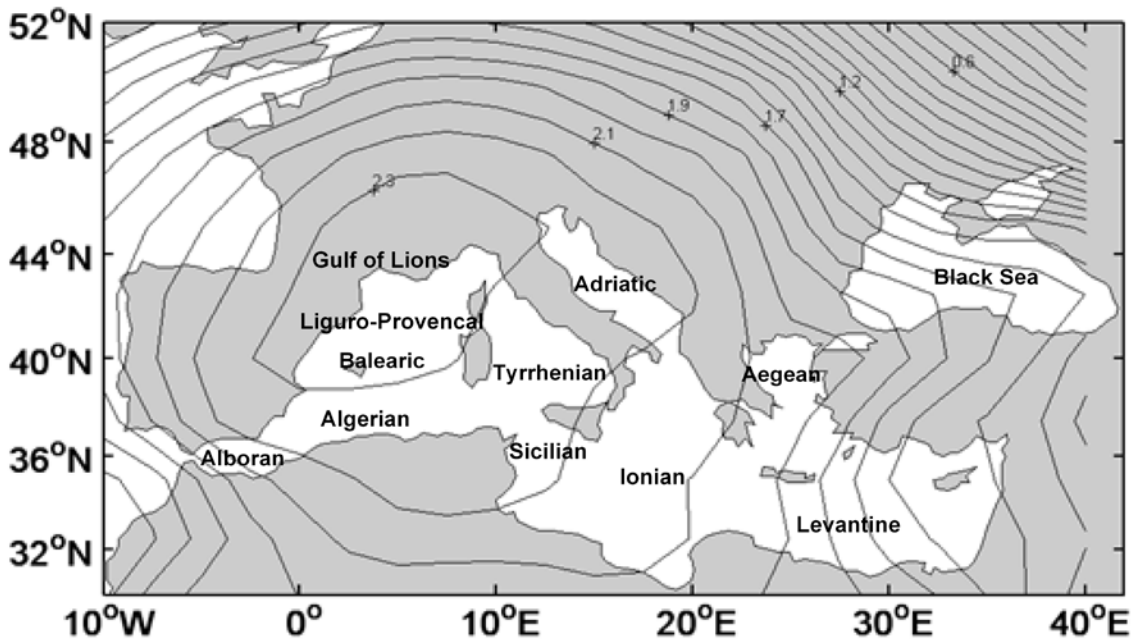
682

683

684

685 **FIGURES**

686



687

688

689 **Figure 1:** Map of the Mediterranean Sea. The main basins and sub-basins are indicated.

690 The MO pattern (contours) has been computed as the first PC of normalised sea level

691 pressure anomalies across the extended Mediterranean region (30°W-40°E, 30°N-60°N).

692

693

694

695

696

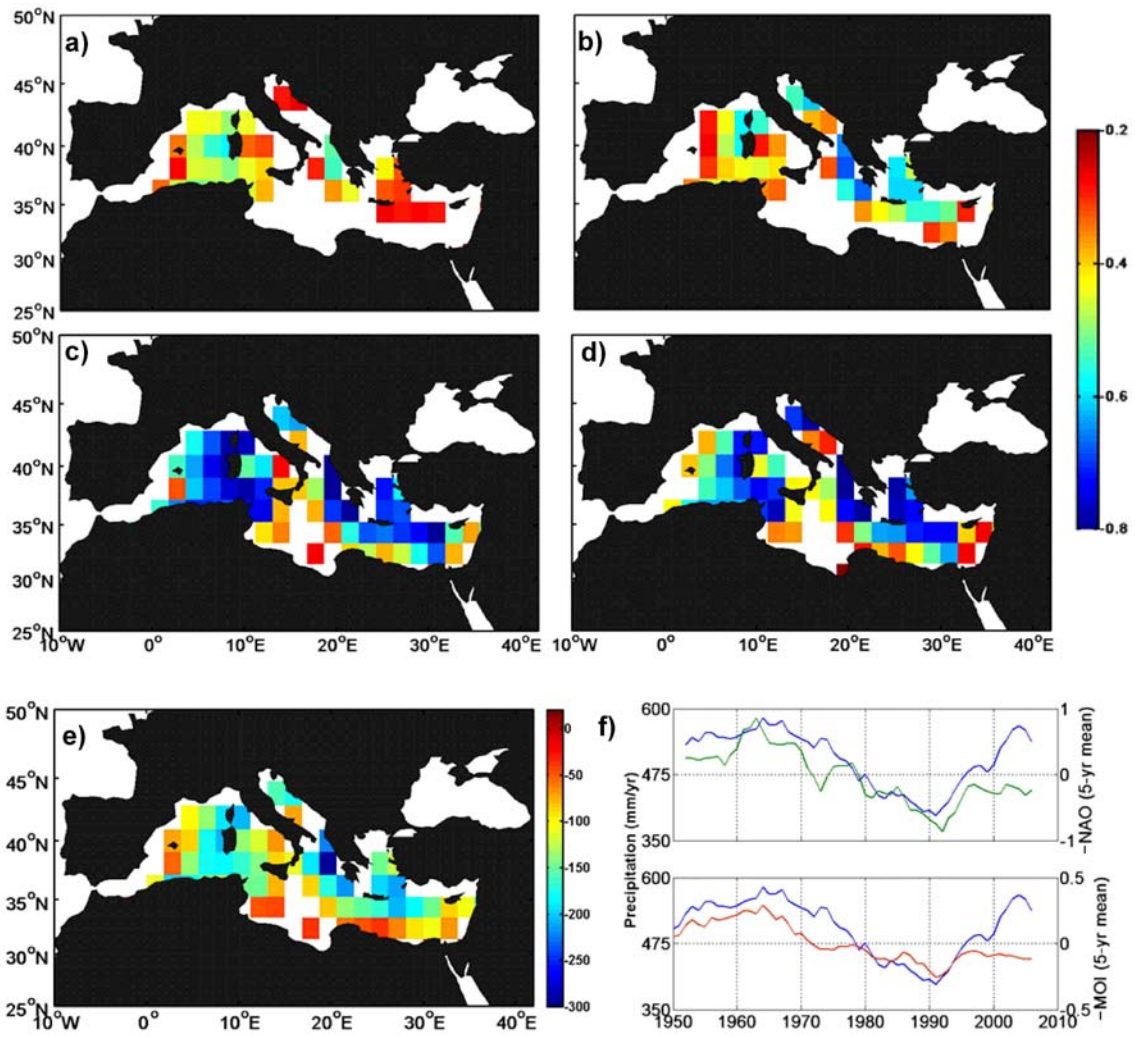
697

698

699

700

701



703

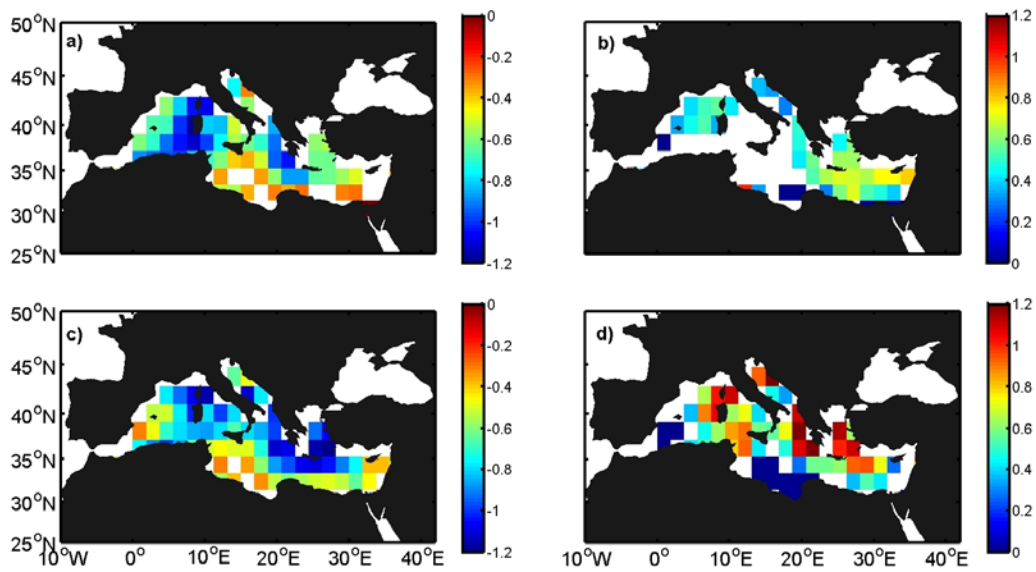
704

705 **Figure 2:** Correlation (95% significance) between precipitation (P) and large-
 706 atmospheric indices for the period 1948-2008. A) Annual P and winter NAO index; B)
 707 Annual P and MO index; C) 5-year running means of P and winter NAO index; D) 5-
 708 year running means of P and MO index. E) Regression of P with winter NAO index at
 709 decadal (5-year running means) timescales; F) Time series of 5-year running means of
 710 winter -NAO (upper, green) and annual -MO (lower, red) indices and Mediterranean-
 711 averaged P.

712

713

714



715

716 **Figure 3:** Composites of precipitation standard anomalies associated to the positive
717 (upper quartile) and negative (lower quartile) phases of winter NAO and MO indices for
718 the 60-year 1948-2008 period. A) Positive winter NAO; B) Negative winter NAO; C)
719 Positive MO; D) Negative MO. Only the points where the results are statistically
720 different from zero (according to a *t*-Student test at 95% significance) have been
721 represented.

722

723

724

725

726

727

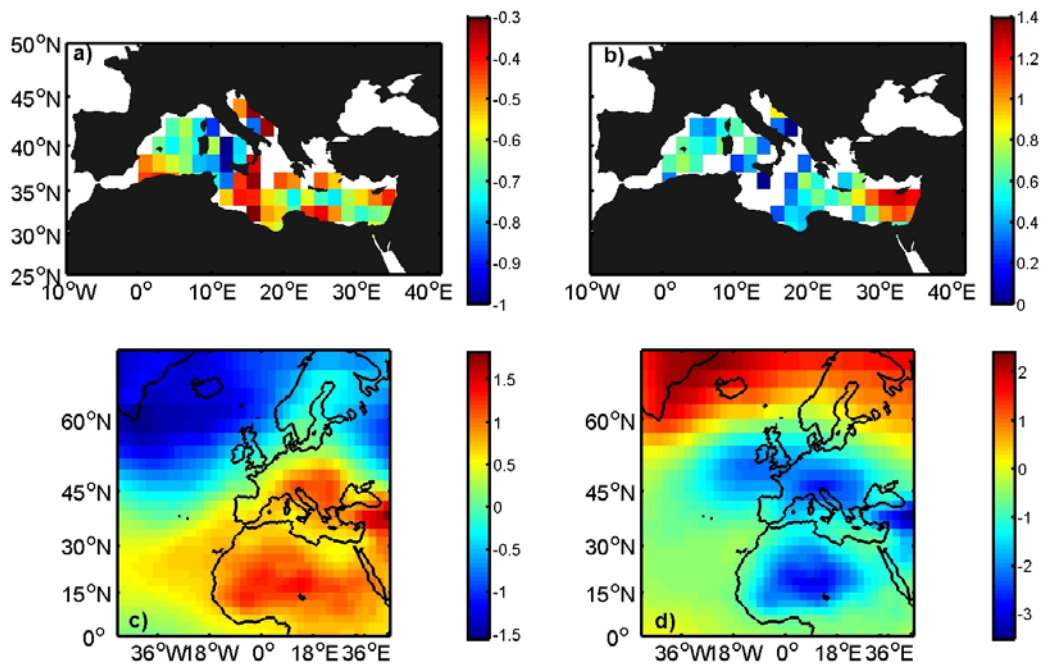
728

729

730

731

732



733

734 **Figure 4:** Composites of evaporation standard anomalies (panels A-B) and sea level
735 pressure anomalies (hPa, panels C-D) associated to the positive (upper quartile, left
736 panels) and negative (lower quartile, right panels) phases of summer MO index for the
737 60-year 1948-2008 period. For evaporation, only the points where the results are
738 statistically different from zero (according to a *t*-Student test at 95% significance) have
739 been represented.

740

741

742

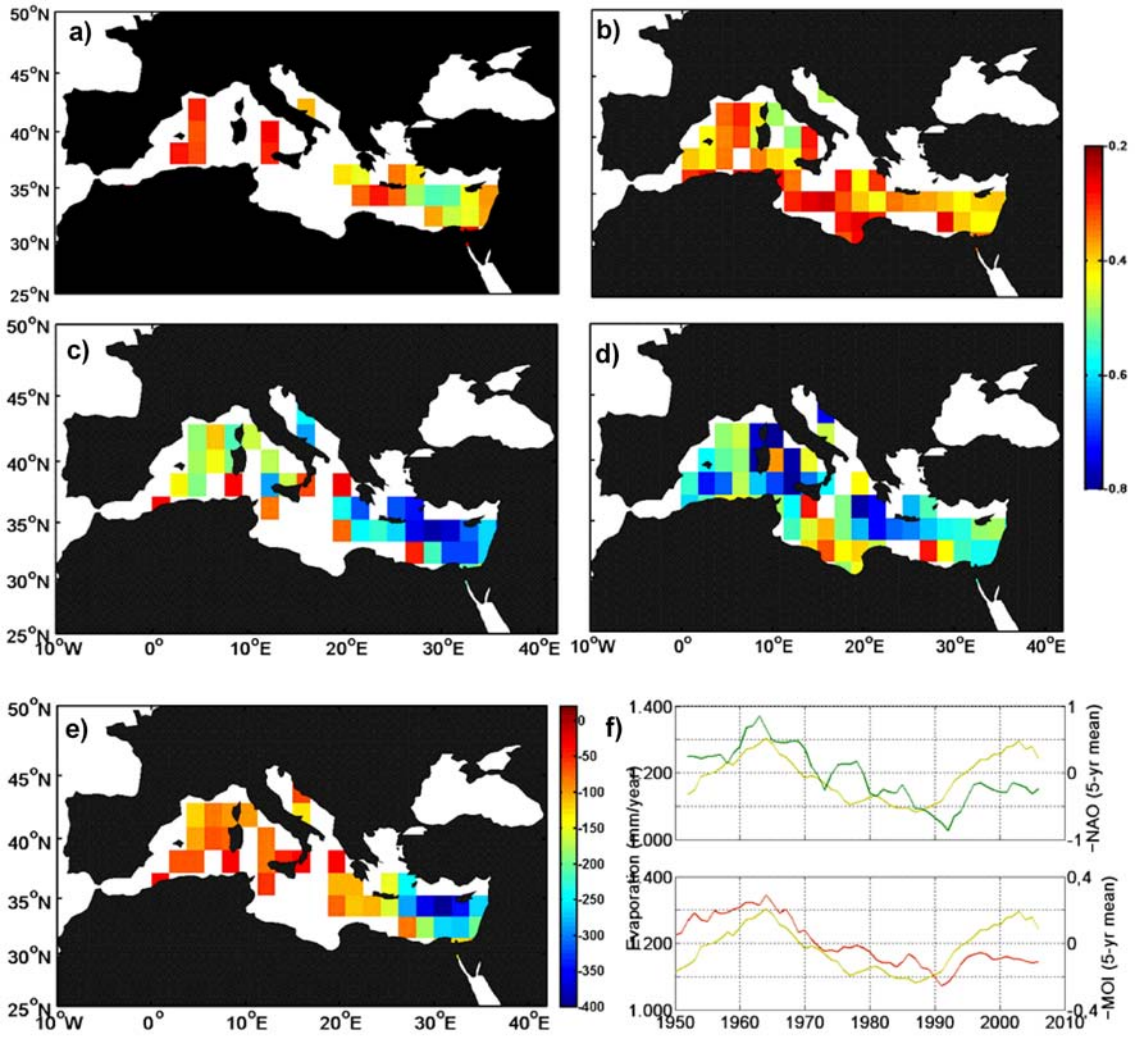
743

744

745

746

747



749

750

751 **Figure 5:** The same as Figure 2 for evaporation. The best correlated summer MO index

752 has been selected for correlations with this variable.

753

754

755

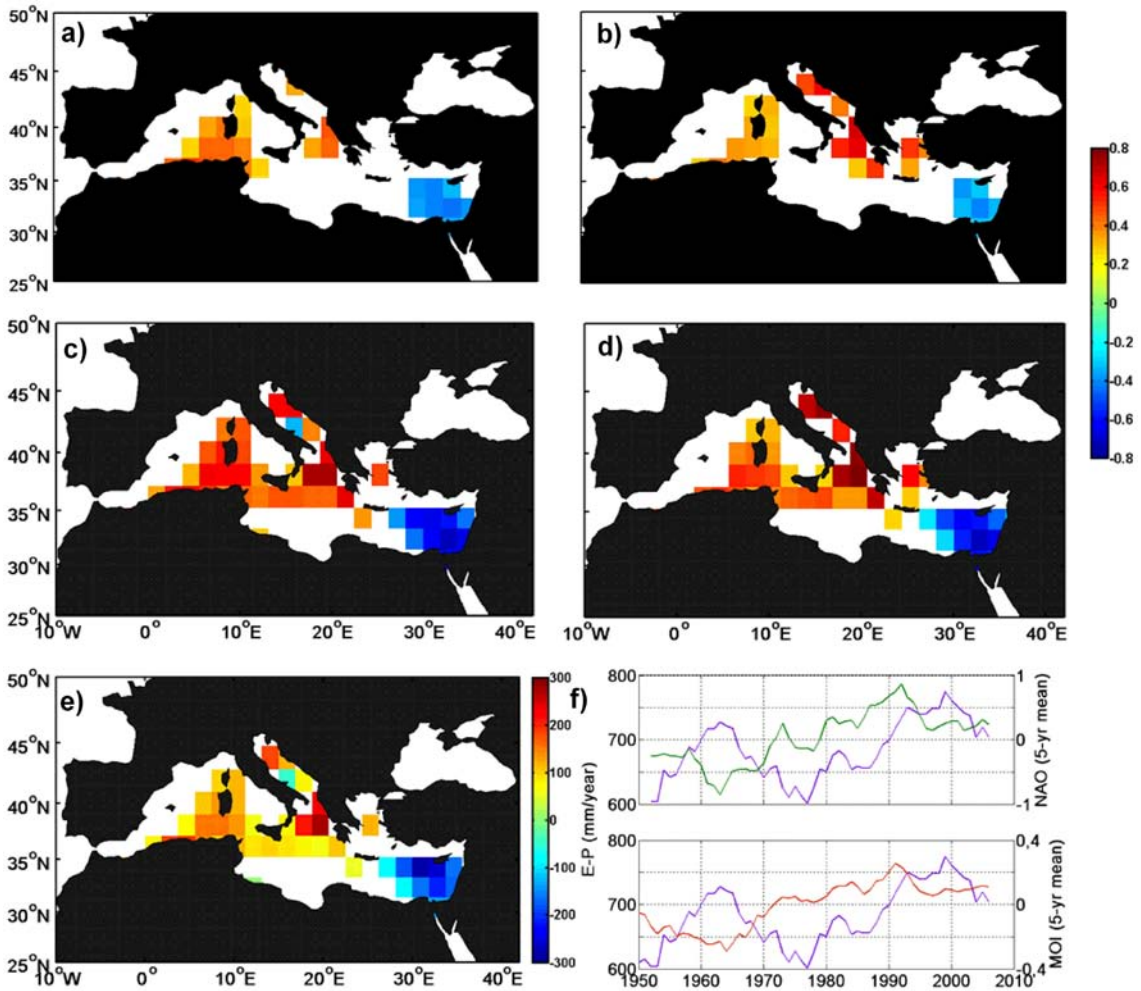
756

757

758

759

760



761

762

763 **Figure 6:** The same as Figure 2 for freshwater deficit E-P. Notice that positive NAO

764 and MO indices have been plotted in panel F.

765

766

767

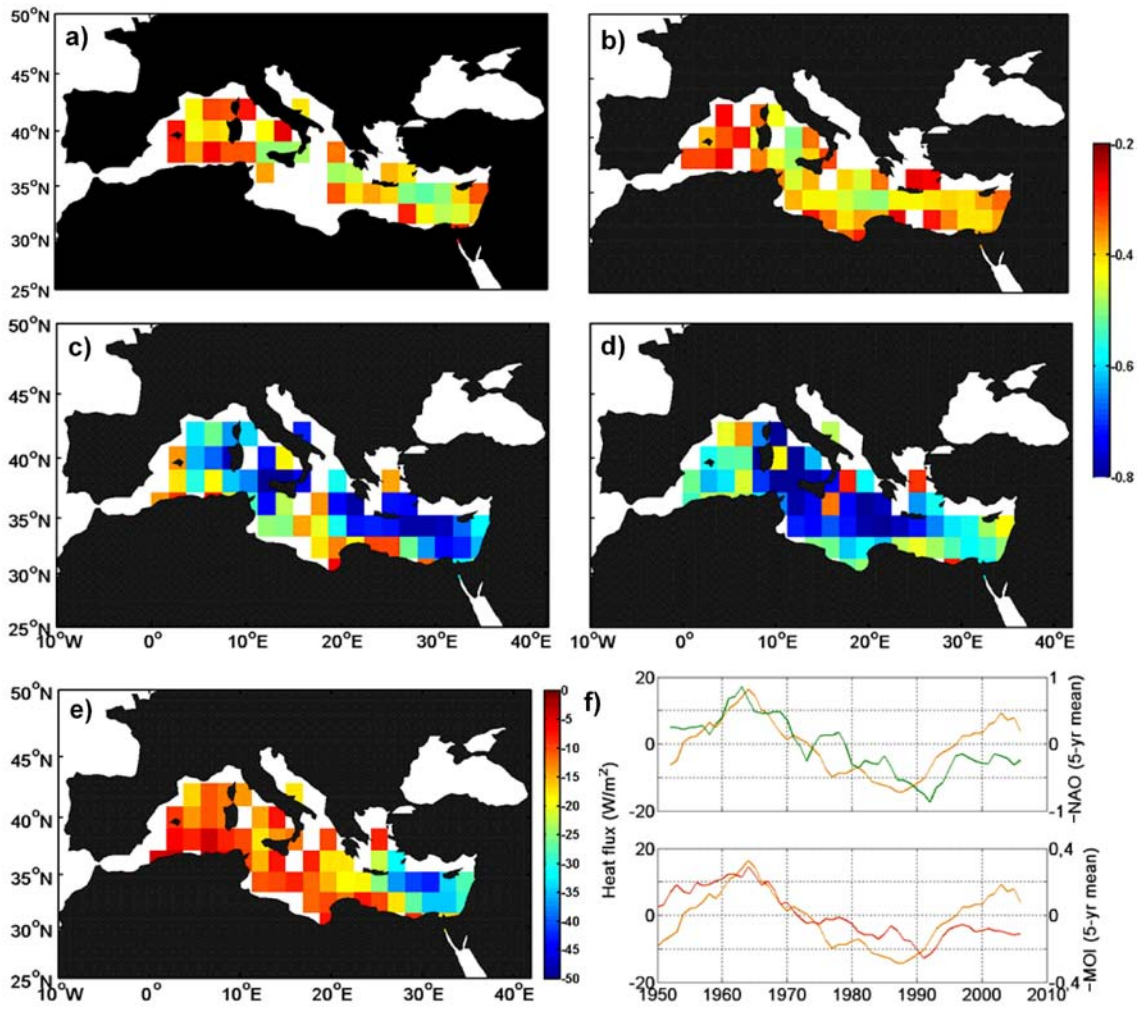
768

769

770

771

772



773

774

775 **Figure 7:** The same as Figure 2 for net heat flux Q . The best correlated summer MO

776 index has been selected for correlations with this variable.

777

778

779

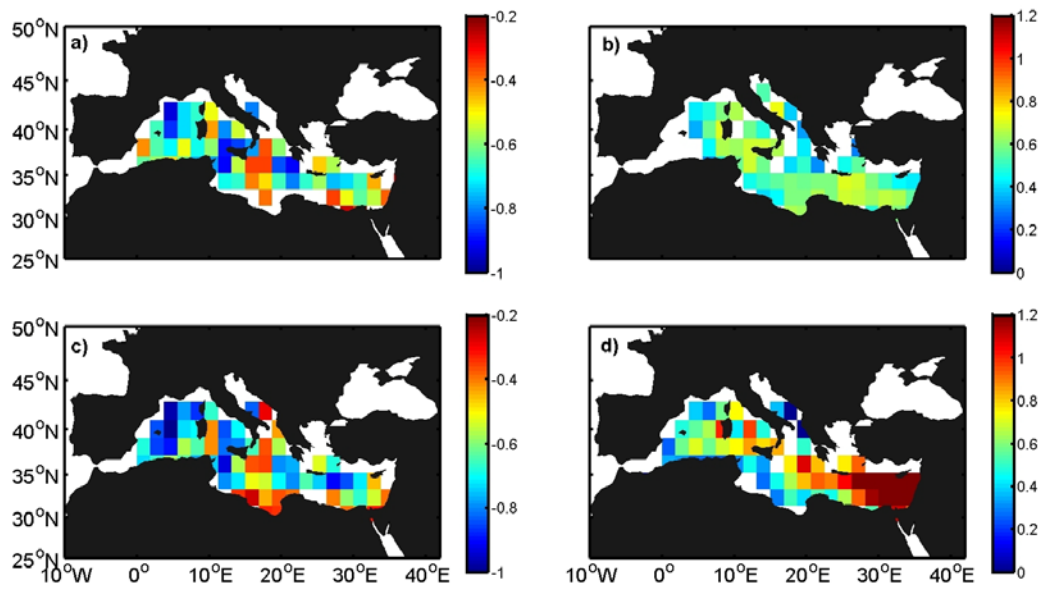
780

781

782

783

784



785

786 **Figure 8:** Composites of net heat flux standard anomalies associated to the positive
787 (upper quartile) and negative (lower quartile) phases of winter NAO and summer MO
788 indices for the 60-year 1948-2008 period. A) Positive winter NAO; B) Negative winter
789 NAO; C) Positive summer MO; D) Negative summer MO. Only the points where the
790 results are statistically different from zero (according to a *t*-Student test at 95%
791 significance) have been represented.

792